

QCD CRITICAL POINT AND HYDRODYNAMIC FLUCTUATIONS IN RELATIVISTIC FLUIDS*

MIKHAIL STEPHANOV

Department of Physics and Laboratory for Quantum Theory at the Extremes
University of Illinois, Chicago, IL 60607, USA

and

Kadanoff Center for Theoretical Physics, University of Chicago
Chicago, IL 60637, USA

*Received 3 March 2024, accepted 10 April 2024,
published online 25 April 2024*

These lecture notes consist of two major connected parts. The first part (Sections 1 and 2), after a brief historical introduction, deals with the physics of critical points in thermodynamic *equilibrium*. The features of the fluctuations relevant to the QCD critical point search are highlighted. The second part (Sections 3 and 4) focuses on the recent developments in the description of the fluctuation *dynamics* especially relevant to the QCD critical point search in heavy-ion collisions.

DOI:10.5506/APhysPolB.55.5-A4

1. Introduction

Almost exactly 200 years ago, Cagniard de la Tour performed an experiment which led to the discovery of critical points in a number of liquids [1]. One can think about this groundbreaking experiment as an attempt to address the following question: What happens if a liquid is heated in a sealed container to such (temperature and pressure) conditions that its propensity to evaporate competes with its propensity to expand, as illustrated in Fig. 1.

Cagniard de la Tour discovered that the boundary (meniscus) separating liquid and gas phases disappears. This phenomenon occurred for all liquids he experimented with, including water. He also described the phenomenon now called *critical opalescence*.

Michael Faraday, at the time, was working on the problem of liquefying gases — his report on the liquefaction of chlorine appears in the same issue as the English translation of Cagniard de la Tour's article [1]. Faraday took great interest in Cagniard de la Tour's discovery, in particular, in its

* Presented at the LXIII Cracow School of Theoretical Physics *Nuclear Matter at Extreme Densities and High Temperatures*, Zakopane, Poland, 17–23 September, 2023.

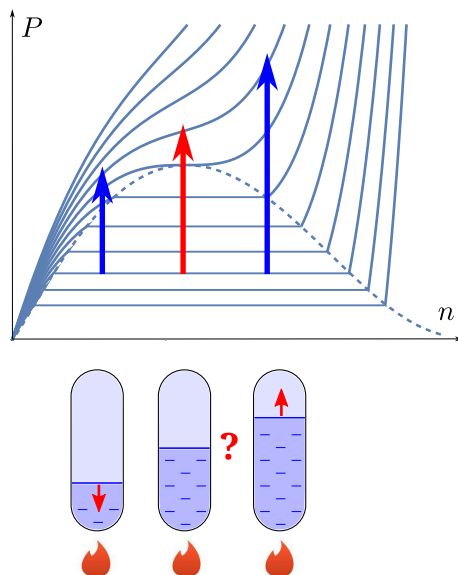


Fig. 1. A schematic representation of Cagniard de la Tour’s experiment, with the heating “histories” indicated by the vertical (fixed volume) lines on the pressure-density diagram (solid lines are isotherms). One can think of this experiment as a (density) scan of the phase diagram. On the left: if a small amount of fluid is placed in a sealed container and heated, the fluid evaporates and the meniscus goes down. On the right: if the fluid fills most of the container, the fluid expands and the meniscus goes up. There must be a certain intermediate, critical filling fraction at which evaporation and expansion compete. What happens to the meniscus at this point?

intriguing implication of the continuity between liquid and gaseous phases. Curiously, Faraday was frustrated that Cagniard de la Tour had not named the novel phenomenon and struggled to come up with a name he needed to refer to a “point at which the fluid and its vapour become one according to a law of continuity” [2].

Full understanding of the ubiquity of the phenomenon and its logical consequence — continuity between “liquid and gaseous states” — was solidified after systematic quantitative studies by Andrews [3], who also coined the name “critical point” we use today.

The desire to explain the liquid–gas continuity and the critical point led Leiden University Ph.D. student van der Waals [4] to discover a model of the equation of state based on, revolutionary at the time, molecular description of matter. The law of corresponding states formulated by van der Waals to describe near-critical fluids paved the way for the concept of universality of critical phenomena.

The phenomenon of critical opalescence was understood by Smoluchowski [5] as an effect of density fluctuations. This discovery was followed by quantitative theoretical description by Einstein [6].

The ubiquity of critical phenomena led Landau to develop the well-known classical theory of phase transitions [7]. But it took much more work to understand the crucial role of fluctuations. This work includes the pioneering contributions by Fisher, Kadanoff, and Wilson, which led to the modern understanding of the (fluctuating) field theory (including quantum field theory) in terms of such essential concepts as scaling and renormalization group.

Thermodynamic critical points are ubiquitous in Nature. Not only practically all fluids possess such a point, but similar phenomena occur in completely different physical systems, such as, *e.g.*, ferromagnets. The universality of critical phenomena extends over a vast range of physically different systems.

Hot and dense QCD matter dominating the Universe moments after the Big Bang, or recreated in heavy-ion collision experiments, is a fluid. It is natural to ask if this fluid also possesses a critical point. This is a non-trivial question first of all because this fluid, unlike the fluids in which critical points have been observed so far, is *relativistic*. In that respect, we are especially interested in the critical point which is related to deconfinement and chiral restoration transition, and we call this point the QCD critical point¹.

There are two necessary prerequisites for the existence of the critical point. One of them is the existence of two phases (*e.g.*, liquid and gas). QCD matter does, indeed, possess such two phases, shown in Fig. 2 — Hadron Resonance Gas (HRG) and Quark–Gluon Plasma (QGP), the latter having liquid properties [9]. Another prerequisite is the continuity between these two phases. Such a continuity has been, indeed, by now rather firmly established by first-principle lattice calculations at zero net baryon density, or $\mu_B = 0$ [10].

Does the crossover separating the two QCD phases at zero μ_B turn into a first-order transition at some finite value of μ_B , and what is that value? *I.e.*, where is the critical point on the QCD phase diagram (see Fig. 2)? Unfortunately, this question cannot, at this time, be answered by a lattice calculation due to the notorious sign problem.

However, this question can be addressed experimentally, by scanning QCD phase diagram in heavy-ion collision experiments [11], as illustrated in Fig. 2. The sought signatures of the critical point are based on the *non-monotonic* dependence of fluctuations on the collision energy, $\sqrt{s_{NN}}$ [8, 12, 13].

¹ The critical point of nuclear matter (see Fig. 2) is also of interest. However, its existence is not in question and its location at temperature of the order of 10 MeV (commensurate with the binding energy of nuclear matter), much smaller than nucleon rest energy, makes it somewhat similar to non-relativistic liquid–gas critical points.

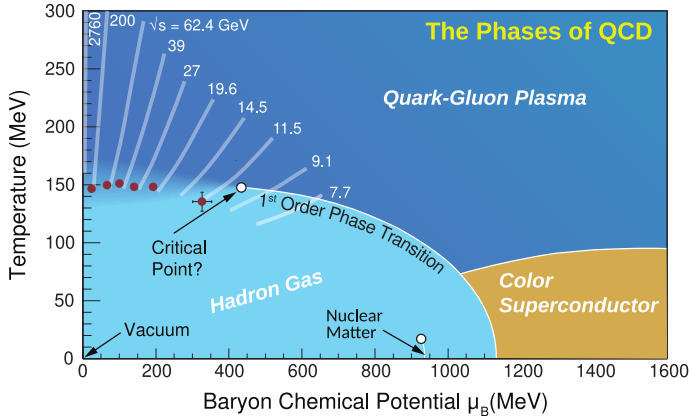


Fig. 2. A schematic rendering of the QCD phase diagram as it is currently understood or conjectured [8]. Superimposed are expansion “histories” of fireballs created in heavy-ion collisions at varying energies used in the beam energy scan experiments (white lines labeled $\sqrt{s_{NN}}$ in GeV). The experimental freezeout points (red) illustrate the dependence of the freezeout point on $\sqrt{s_{NN}}$.

While fluctuations in thermodynamic *equilibrium* near critical points, and their role in such critical phenomena as critical opalescence have been long and well understood, heavy-ion collisions present an additional challenge — fluctuation dynamics.

The QCD matter (QGP) fireball created in heavy-ion collisions evolves sufficiently slowly that it can be described by hydrodynamics. However, the separation of scales is not astronomical, as in usual condensed matter contexts. As a result, fluctuations, which take time to relax to evolving equilibrium during the expansion, could deviate substantially from equilibrium values at freezeout.

After a brief introduction to equilibrium fluctuations (which can be also found elsewhere, *e.g.*, [8]), these lectures will describe the recent progress achieved in the dynamical description of fluctuations.

2. Fluctuations in thermodynamics, critical fluctuations

2.1. Relation between equation of state and fluctuations

In thermodynamic equilibrium (by definition), the probability of the system to be found in a given *microscopic*, *i.e.*, quantum, state depends only on the conserved quantum numbers of this state, such as energy, momentum, charge, *etc.* Therefore, the probability of a given *macroscopic* state, characterized by a given set of macroscopic variables, such as energy, is proportional to the number of microscopic states with these values of the

macroscopic variables. That probability is equal to the exponential of the entropy, by definition. Therefore, the dependence of the entropy on energy, *etc.*, *i.e.*, the equation of state (EoS), determines the probability of the fluctuations for a system in thermodynamic equilibrium [14].

This fundamental relationship between fluctuations and EoS is at the core of Einstein's description [6] of the density fluctuations, whose singular behavior near critical points explains the phenomenon of critical opalescence [5].

The entropy in question is the entropy of the open system which can exchange conserved quantities, such as energy and charge with the surroundings (thermodynamic bath) at temperature T and chemical potential μ . The corresponding probability distribution for the values of energy density ϵ and charge density n is given by

$$\mathcal{P}(\epsilon, n) \sim \exp \{V[s(\epsilon, n) - \beta\epsilon + \alpha n]\} , \quad (1)$$

where $\beta = 1/T$, $\alpha = \mu/T$, and V is the volume of the thermodynamic system. In the thermodynamic limit, *i.e.*, for large V , the probability is sharply peaked around the maximum determined by the familiar conditions

$$\left(\frac{\partial s}{\partial \epsilon}\right)_n - \beta = 0, \quad \left(\frac{\partial s}{\partial n}\right)_\epsilon + \alpha = 0. \quad (2)$$

I.e., the entropy $s(\epsilon, n)$ determines the relationship between conserved densities ϵ , n , and the corresponding thermodynamic quantities T and μ .

The quadratic form of second derivatives of the entropy must be negative to ensure thermodynamic stability. This form can be diagonalized using variables $m \equiv s/n$ (specific entropy) and p (pressure). The probability of small fluctuations in terms of these variables is given by

$$\mathcal{P} \sim \exp \left\{ -\frac{V}{2} \left(\frac{n^2}{c_p} (\delta m)^2 + \frac{\beta}{wc_s^2} (\delta p)^2 + \dots \right) \right\} , \quad (3)$$

where $c_s^2 = (\partial p / \partial \epsilon)_m$ and $w = \epsilon + p$.

Specific heat $c_p = Tn(\partial m / \partial T)_p$ diverges at the critical point. This corresponds to the probability of fluctuations developing a “flat direction” along which $\delta p = 0$, where the fluctuations of the specific entropy $V\langle(\delta m)^2\rangle = c_p/n^2$ become large². The non-monotonic behavior of fluctuations as the

² Other thermodynamic quantities also develop large fluctuations at the critical point. For example, $V\langle(\delta n)^2\rangle = \chi_T T$, where $\chi_T = (\partial n / \partial \mu)_T$ is also divergent. The specific entropy $m = s/n$ is special from the hydrodynamic point of view. Unlike, *e.g.*, baryon density, $m = s/n$ is a normal hydrodynamic mode in ideal hydrodynamics, *i.e.*, being a ratio of conserved densities specific entropy is a diffusive mode which does not mix with propagating sound modes.

critical point is being approached and passed during the QCD phase diagram scan has been proposed as a signature of the QCD critical point [12, 15].

Before proceeding, let us pause to note that in these lectures, we focus on the fluctuations intrinsic in any system which affords local thermodynamic, statistical description. These fluctuations are determined by the equation of state, as discussed above. In the context of heavy-ion collisions, we must distinguish these fluctuations from the fluctuations which are determined by the initial state of the system. For example, from the fluctuations of the initial geometry of the system. In experiments, such separation is not always trivial. Typically, it involves selecting collisions with similar centrality, *i.e.*, similar collision geometry. The effects of the initial fluctuations are also qualitatively different from those of thermodynamic fluctuations in that the correlations induced by initial fluctuations are longer range (in longitudinal rapidity space) than the thermodynamic fluctuations we discuss [16]. Most importantly, the $\sqrt{s_{NN}}$ dependence of the initial fluctuations does not reflect the *non-monotonicity* inherent in the thermodynamic fluctuations in the vicinity of the critical point.

2.2. Universality and non-Gaussianity of critical fluctuations

Since the equation of state is universal near critical points, the fluctuation phenomena are also universal. In this section, we shall describe some universal properties of the fluctuations which are relevant to the search for the QCD critical point in heavy-ion collisions.

Since the coefficient of the $(\delta m)^2$ term in Eq. (3) vanishes at the critical point, non-Gaussian terms in Eq. (3), such as δm^3 , δm^4 , *etc.*, become important. This makes non-Gaussianity of fluctuations a telltale signature of the critical point [17].

Similarly, the vanishing of the coefficient of δm^2 in Eq. (3) makes gradient terms, such as $(\nabla \delta m)^2$, important and leads to the divergence of the correlation length ξ of the fluctuations at the critical point. The non-Gaussianity of fluctuations and the divergence of the correlation length go hand in hand since the limit $V/\xi^3 \rightarrow \infty$, which ensures the Gaussianity of the fluctuations via the central limit theorem, is in obvious conflict with $\xi \rightarrow \infty$.

The fluctuations at length scales of the order of the correlation length cannot be described by the variable δm , or by the uniform “mean field” δm , alone. Instead, the fluctuating spatially varying field $\delta m(x)$ must be considered. The corresponding scalar field theory — ϕ^4 theory in three dimensions — is universal in that it describes a wide range of critical phenomena from liquid–gas critical points to uniaxial (Ising) ferromagnets. The full details of the universal theory of critical phenomena are beyond the scope of these lectures, and are covered in many textbooks and reviews on critical phenom-

ena [18, 19]. Here, we shall emphasize only the basic properties which are most relevant to the critical point search in the beam-energy scan heavy-ion collision experiments.

The universality means that we can consider fluctuations of m , or any other quantity, whose fluctuations diverge at the critical point, such as baryon number or entropy density (and in the case of ferromagnets, magnetization density) as an order parameter and map it onto the field variable ϕ in the ϕ^4 theory, *i.e.*,

$$\Delta m \equiv m - m_c \sim \phi, \quad (4)$$

where m_c is the value of m at the critical point and the implicit coefficient of proportionality is determined by the normalization of the field ϕ . The universality of the critical point phenomena means that the probability of fluctuations can be expressed in terms of the field ϕ

$$\mathcal{P}[\phi] \sim \exp \left\{ -V \left(-h\phi + \frac{r}{2}\phi^2 + \frac{\lambda}{4}\phi^4 + \frac{1}{2}(\nabla\phi)^2 \dots \right) \right\}, \quad (5)$$

where we expanded in powers of ϕ and kept the leading non-Gaussian term ϕ^4 as well as the leading gradient term $(\nabla\phi)^2$. At the critical point, the ordering field h and the reduced temperature r vanish. The probability becomes non-Gaussian and, at the same time, the correlation length ξ , proportional to $r^{-1/2}$ in the mean-field approximation (*i.e.*, neglecting fluctuations), diverges. The cumulants of the order parameter ϕ also diverge, according to

$$\langle \phi^2 \rangle \sim \xi^2, \quad \langle \phi^3 \rangle \sim \xi^{4.5}, \quad \langle \phi^4 \rangle^c \sim \xi^7, \quad (6)$$

with (approximate) powers different from mean-field values due to fluctuations. Here and below “c” stands for “cumulant”, *i.e.*, $\langle \phi^4 \rangle^c = \langle \phi^4 \rangle - 3\langle \phi^2 \rangle^2$.

It is important that, unlike the variance $\langle \phi^2 \rangle$, which measures the width of the probability distribution, the cubic and quartic cumulants, which measure the shape, are not positive definite. The cubic cumulant, measuring the skewness of the probability distribution \mathcal{P} , has the sign determined by the sign of h . The sign of the quartic cumulant can be understood by looking at the value of the cumulant along the crossover line $r > 0$ at $h = 0$, as illustrated in Fig. 3. The distribution along this line starts off as Gaussian away from the critical point and then splits into two maxima on the phase coexistence (first-order phase transition) line for $r < 0$. As $r \rightarrow +0$, the distribution becomes “flatter” which is represented by the negative value of the quartic cumulant³.

³ The quartic cumulant is related to kurtosis, K : $K = \langle \phi^4 \rangle^c / \langle \phi^2 \rangle^2$, which has an advantage of canceling the overall normalization of ϕ .

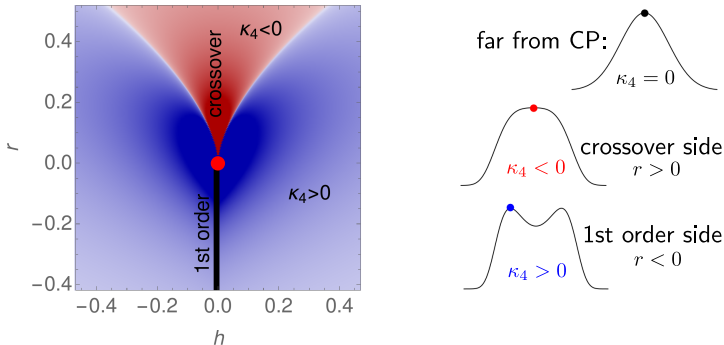


Fig. 3. Left: The sign of the quartic cumulant $\kappa_4 \equiv \langle \phi^4 \rangle^c$ as a function of ϕ^4 (Ising model) field theory parameters h and r . Right: Schematic representation of the probability distribution $\mathcal{P}[\phi]$ in Eq. (5) at different points on the $h = 0$ line.

For $r < 0$, on the coexistence line, while the distribution is symmetric, the symmetry is spontaneously broken and the fluctuations occur around one of the maxima. This skewness effect dominates the quartic cumulant making it positive (see, *e.g.*, [20] for more details).

The linear mapping from the Ising model variables h and r and the QCD variables μ and T captures the singular behavior of the QCD thermodynamics due to the fluctuations of the order parameter field ϕ , as well as due to the next-to-leading relevant operator (ϕ^2 in the mean-field approximation) [21–23].

Such a mapping has been standardized in Ref. [24] using 6 parameters: T_c , μ_{Bc} , w , ρ , α_1 , and α_2 . The parameters T_c and μ_{Bc} set the location of the QCD critical point, while α_1 is the angle of the slope of the coexistence line (first-order phase transition line) at the critical point in the T versus μ_B plane. It is also the slope of $m = m_c$ (critical isentrope) line at the critical point and is obtained by mapping the zero magnetization line $\phi = 0$ (*i.e.*, zero magnetic field $h = 0$) of the Ising model onto the QCD phase diagram. The angle α_2 is the angle of the line on the QCD phase diagram onto which the constant temperature line passing through the Ising critical point maps.

The non-Gaussian cumulants of the order parameter such as m are proportional to those in the Ising model (or ϕ^4 theory, see Eq. (4)), but mapped onto the QCD phase diagram. In particular, these cumulants contain singular contributions which diverge at the critical point with universal powers of the correlation length, given approximately by [17]

$$\Delta \langle (\delta m)^2 \rangle \sim \xi^2, \quad \Delta \langle (\delta m)^3 \rangle \sim \xi^{4.5}, \quad \Delta \langle (\delta m)^4 \rangle^c \sim \xi^7, \quad (7)$$

where Δ reminds us that this is a *contribution* to cumulants, singular at the critical point. There are, of course, less singular and regular contributions, or baseline. The search for the critical point is aimed at detecting the

non-monotonic dependence of fluctuations measures on the collision energy $\sqrt{s_{NN}}$ as the critical point is approached and passed, *i.e.*, as the correlation length increases and then shrinks back to non-critical background, or baseline, values.

For example, the quartic cumulant around the QCD critical point is illustrated in Fig. 4 (a) [20]. The resulting dependence on the collision energy, as it is varied in the region where the freeze-out occurs near the critical point, is illustrated in Fig. 4 (b). The characteristic non-monotonicity of this cumulant is one of the signatures of the critical point searched for in the beam energy scan experiments [8].

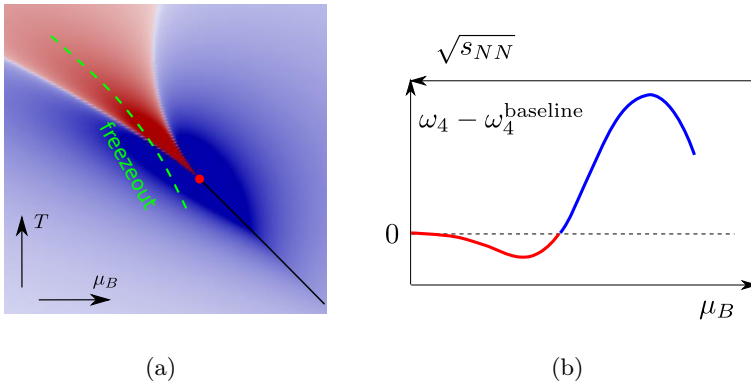


Fig. 4. The equilibrium expectation for the quartic cumulant of fluctuations as a function of temperature and baryon chemical potential on the QCD phase diagram in the vicinity of the critical point. Red and blue colors reflect the sign of the cumulant — negative and positive respectively. Compare to Fig. 3. The sign changes as the QCD phase diagram is scanned by varying $\sqrt{s_{NN}}$, and thus T and μ_B , along the freeze-out “trajectory” (dashed green line).

The most recently published experimental measurements of quartic cumulants by the STAR Collaboration indicate a non-monotonic dependence of the type similar to the one shown in Fig. 4 (b) (see, *e.g.*, Fig. 4(2) in Ref. [25]). While the magnitude of the cumulant sensitively depends on the EoS, and thus is hard to predict (hence the lack of the vertical scale in Fig. 4 (b)), the experimental results indicate that monotonic dependence is excluded at 3.1σ level [25–27]. While not yet a definitive indication of the presence of the QCD critical point, this intriguing result motivates the second phase of the beam energy scan (BES-II) program which has collected higher statistics data being processed and analyzed currently.

We shall focus on the recent progress achieved in connecting these equilibrium fluctuations to the experimental measurements. There are at least two steps that need to be made to get from the equilibrium thermodynamic fluctuations to the experimental observables:

First, like thermodynamic variables themselves, the fluctuations of these variables evolve. This evolution is subject to conservation laws which may lead to significant memory effects, *i.e.*, the lag of the fluctuations behind the instantaneous equilibrium values.

Second, the thermodynamic/hydrodynamic quantities are not measured by experiments directly. An important step is connecting the fluctuations of these quantities to the observables, such as measures of particle multiplicity fluctuations and correlations.

The following two sections will review the recent development towards accomplishing these two steps necessary for connecting the theory and the experiment.

3. Fluctuations in hydrodynamics

3.1. Stochastic hydrodynamics

There has been significant recent progress in understanding and describing the *dynamics* of local thermodynamic fluctuations in hot *relativistic* fluids, such as the QCD matter making up a heavy-ion collision fireball.

The evolution of the QCD matter in the heavy-ion fireball is successfully described in the framework of hydrodynamics. This description is inherently statistical, and therefore, fluctuations are an essential part of this description. One can also understand this fact by invoking fluctuation–dissipation theorem according to which dissipative systems (such as non-ideal hydrodynamics) have to be stochastic.

There are two complementary approaches for describing dynamics of fluctuations, which we shall refer to as stochastic and deterministic. Both begin with the Landau–Lifshits theory of hydrodynamic fluctuations [28]. In this theory, generalized to a relativistic context in Ref. [16], the equations of hydrodynamics are *stochastic*.

The hydrodynamic description exists due to the separation of scales. The timescale of relaxation to local equilibrium (typical microscopic time, such as inter-collision time) is much shorter than the time needed to transport conserved quantities and establish global equilibrium. This is typically a diffusion time proportional to the square of the size of inhomogeneities in the system. This latter slow evolution process is essentially governed by conservation equations, which we can write generically as

$$\partial_\mu \tilde{J}^\mu = 0 \tag{8}$$

by combining all conserved currents into an array

$$\check{\mathcal{J}}^\mu \equiv \left\{ \check{N}_q^\mu, \check{T}^{\mu\nu} \right\}. \quad (9)$$

We use the ‘breve’ accent to denote stochastic (fluctuating) quantities. For QCD, such conserved currents include currents of energy and momentum, $T^{\mu\nu}$, as well as conserved charge currents, N_q^μ , among which we shall focus on the baryon charge $q = B$.

While each current involves one time and three spatial components, there is only one equation for each current in (8). Therefore, to close the system of equations, we need to express all 4 current components in terms of 1 variable — the conserved density. To maintain relativistic covariance, we want this density to be a covariant object (scalar for the baryon charge density, or vector for energy-momentum density). The density in the lab frame would not do.

The fluid itself, however, allows us to define (in each space-time point) a reference frame associated with fluid’s motion. This frame is often referred to as the “local rest frame” of the fluid. Following Landau, we chose for that purpose the frame in which the momentum density vanishes. The 4-velocity of such a frame solves the following equation (known as “Landau condition”):

$$\check{T}^\mu_\nu \check{u}^\nu = \check{\epsilon} \check{u}^\mu. \quad (10)$$

Since \check{T}^μ_ν fluctuates, so does \check{u}^μ . Equation (10) also defines the energy density $\check{\epsilon}$ in the fluid’s rest frame. The rest frame charge density is defined similarly $\check{n}_q = \check{u}_\mu \check{N}_q^\mu$.

It is convenient to define an array of these covariant variables — one for each conservation equation in (8)

$$\check{\Psi} \equiv \check{u}_\mu \check{\mathcal{J}}^\mu = \{ \check{n}_q, \check{\epsilon} \check{u}^\nu \}. \quad (11)$$

In order to close the system of equations, we need to express all components of the currents in $\check{\mathcal{J}}^\mu$ in terms of the covariant variables in $\check{\Psi}$. The separation of scales in hydrodynamics means that this relationship is *local*. I.e., the currents $\check{\mathcal{J}}(x)$ are functions of variables $\check{\Psi}(x)$ and its gradients at the same point x

$$\mathcal{J}^\mu[\Psi] = \{ n u^\mu, \epsilon u^\mu u^\nu - p(g^{\mu\nu} - u^\mu u^\nu) \} + \text{diffusive/viscous gradients}. \quad (12)$$

The key point of the Landau–Lifshits theory of hydrodynamic fluctuations is that the constitutive relations such as (12) are only satisfied *on average* — hence the absence of the ‘breve’ in Eq. (12). For fluctuating quantities, there is a random discrepancy, which is due to the microscopic degrees of freedom excluded from the hydrodynamic description. Hence,

$$\check{\mathcal{J}}^\mu = \mathcal{J}^\mu \left[\check{\Psi} \right] + \check{\mathcal{I}}^\mu, \quad (13)$$

where $\check{\mathcal{I}}^\mu$ is the local noise, $\langle \check{\mathcal{I}}^\mu \rangle = 0$, whose correlation function,

$$\langle \check{\mathcal{I}}^\mu(x_1) \check{\mathcal{I}}^\nu(x_2) \rangle \sim \delta^{(4)}(x_1 - x_2), \quad (14)$$

is determined by the fluctuation–dissipation theorem, ensuring that the equilibrium fluctuations and correlations have the correct magnitudes in agreement with thermodynamics.

The evolution of fluctuations can be then described by, for example, directly solving this system of stochastic equations (8) and (13). In a numerical simulation, this *stochastic* approach, however, produces a problem (also known as infinite noise problem) due to the fact that the noise is singular at $x_1 = x_2$ in Eq. (14). The resulting solutions are dependent on the hydrodynamic cutoff, *i.e.*, the finite elementary hydrodynamic cell size, b , complicating the “continuum limit” $b \rightarrow 0$. Some solutions to this problem within a numerical simulation have been proposed and implemented in the literature [29, 30], but we shall not discuss them here.

3.2. Deterministic approach to hydrodynamic fluctuations

The approach which deals with the infinite noise problem *before* the actual numerical simulation is performed has been also developed recently for Bjorken flow [31–33], for arbitrary relativistic flow [34–36], and for non-Gaussian fluctuations [37, 38]. In this *deterministic* approach, one expands in fluctuations around the average $\Psi \equiv \langle \check{\Psi} \rangle$

$$\check{\Psi} = \Psi + \delta\Psi, \quad (15)$$

thus obtaining stochastic equations for the fluctuations $\delta\Psi$ on the deterministically evolving inhomogeneous fluctuation averaged background $\Psi(x)$. These equations can then be used to derive *deterministic* equations obeyed by the *correlation functions* of the fluctuations, *i.e.*, by averages of the products of the fluctuations, such as $\langle \delta\Psi(x_1) \delta\Psi(x_2) \rangle$.

The short-distance singularity of the noise results in ultraviolet divergences in the deterministic equations — the infinite noise problem. Indeed, expanding constitutive equations (13) to quadratic order and averaging, one finds

$$\langle \check{\mathcal{J}}^\mu(x) \rangle = \mathcal{J}^\mu[\Psi(x)] + \frac{1}{2} \frac{\partial^2 \mathcal{J}^\mu}{\partial \Psi_a \partial \Psi_b} \langle \delta\Psi_a(x) \delta\Psi_b(x) \rangle + \dots, \quad (16)$$

where a, b index hydrodynamic variables in the array (11). The last term in Eq. (16) is singular because the correlator of hydrodynamic variables is evaluated at coinciding points, and in (and near) equilibrium $\langle \delta\Psi_a(x_1) \delta\Psi_b(x_2) \rangle \sim$

$\delta(x_1 - x_2)$. The support of the delta function is of the size of the hydrodynamic cell b , over which the operators defining conserved densities are averaged to obtain classical (stochastic) hydrodynamic variables $\tilde{\Psi}$.

The key observation is that these singular (divergent in the limit $b \rightarrow 0$) contributions are *local* due to the hydrodynamic separation of scales we discussed already. Thus, the divergent terms in Eq. (16) must simply renormalize the local terms already present in the “bare” constitutive relations in Eq. (12). The resulting system of renormalized equations for hydrodynamic evolution of the renormalized average densities, as well as the correlation functions, is ultraviolet finite, *i.e.*, cutoff independent, and the continuum limit can be taken (see, Refs. [35, 36] for more detail).

After the renormalization, the averaged hydrodynamic equations keep the form of usual hydrodynamic equations to the first order in gradients with renormalized, *i.e.*, physical, equation of state and transport coefficients. However, finite (*i.e.*, cutoff-independent) fluctuation contributions appear beyond that order. These terms introduce contributions non-local in space (effectively being of order 3/2 in gradients) and also non-local in time, leading to the phenomena known as “long-time tails”. Near the critical point, these fluctuation effects also lead to critical slowing down of the relaxation to equilibrium [34] and the related divergence of kinetic coefficients, most notably, of bulk viscosity [34, 36, 39].

3.3. Multipoint Wigner transform

Since fluctuations occur on shorter length scales than the hydrodynamic evolution of the background [31, 34, 35], it is convenient to consider Wigner-transformed equal-time correlation functions. For a fluid at rest globally, the Wigner transform definition is straightforward

$$W_{ab}(t, \mathbf{x}; \mathbf{q}) = \int d^3\mathbf{y} \left\langle \delta\Psi_a \left(t, \mathbf{x} + \frac{\mathbf{y}}{2} \right) \delta\Psi_b \left(t, \mathbf{x} - \frac{\mathbf{y}}{2} \right) \right\rangle e^{-i\mathbf{q}\cdot\mathbf{y}}, \quad (17)$$

where $\delta\Psi_a$ is the fluctuation of a hydrodynamic field from array (11) labeled by index a .

Non-Gaussianity of fluctuations, important for the critical point search, is described by *connected* correlation functions of $k > 2$ fluctuation fields

$$H_{a_1 \dots a_k}(t, \mathbf{x}_1, \dots, \mathbf{x}_k) \equiv \langle \delta\Psi_{a_1}(t, \mathbf{x}_1) \dots \delta\Psi_{a_k}(t, \mathbf{x}_k) \dots \rangle^{\text{connected}}. \quad (18)$$

The corresponding generalization of the Wigner transform was introduced in Ref. [37] in terms of the Fourier integral with fixed midpoint

$$\mathbf{x} \equiv \frac{\mathbf{x}_1 + \cdots + \mathbf{x}_k}{k}, \quad (19)$$

i. e.,

$$\begin{aligned} W_{a_1 \dots a_k}(t, \mathbf{q}_1, \dots, \mathbf{q}_k) &\equiv \int d^3 \mathbf{y}_1 e^{-i \mathbf{q}_1 \cdot \mathbf{y}_1} \dots \int d^3 \mathbf{y}_k e^{-i \mathbf{q}_k \cdot \mathbf{y}_k} \\ &\times \delta^{(3)} \left(\frac{\mathbf{y}_1 + \cdots + \mathbf{y}_k}{k} \right) H_{ab \dots}(t, \mathbf{x} + \mathbf{y}_1, \dots, \mathbf{x} + \mathbf{y}_k). \end{aligned} \quad (20)$$

Due to the delta-function factor in Eq. (20), the function W does not change if all \mathbf{q} s are shifted by the same vector. This means that one of the \mathbf{q} arguments is redundant. In practice, it is sufficient to know the function W at all values of \mathbf{q} which add up to zero. In particular, the correlator $H_{a_1 \dots a_k}$ can be obtained via inverse transformation

$$\begin{aligned} H_{a_1 \dots a_k}(t, \mathbf{x}_1, \dots, \mathbf{x}_k) &= \int \frac{d^3 \mathbf{q}_1}{(2\pi)^3} e^{i \mathbf{q}_1 \cdot \mathbf{y}_1} \dots \int \frac{d^3 \mathbf{q}_k}{(2\pi)^3} e^{i \mathbf{q}_k \cdot \mathbf{y}_k} \\ &\times (2\pi)^3 \delta^{(3)}(\mathbf{q}_1 + \cdots + \mathbf{q}_k) W_{a_1 \dots a_k}(t, \mathbf{x}; \mathbf{q}_1 \dots \mathbf{q}_k), \end{aligned} \quad (21)$$

where $\mathbf{y}_i \equiv \mathbf{x}_i - \mathbf{x}$. For $k = 2$ the generalized Wigner function $W_{ab}(t, -\mathbf{q}, \mathbf{q})$ coincides with the usual 2-point Wigner function defined in Eq. (17).

3.4. Evolution equations for fluctuations in a diffusion problem

The hierarchy of evolution equations was derived in Ref. [37] for fluctuations of density in a diffusion problem, where the only hydrodynamic variable is the diffusing charge density n which obeys the conservation equation and Fick's law with local noise

$$\partial_t n = -\nabla \cdot \mathbf{N}, \quad \mathbf{N} = -\lambda(n) \nabla \alpha(n) + \text{noise}. \quad (22)$$

The evolution equations describe the relaxation of the k -point functions W_k of fluctuations of density n to equilibrium values given by thermodynamics in terms of the equation of state $\alpha(n)$ (chemical potential divided by temperature)

$$\partial_t W_2(\mathbf{q}) = -2 [\gamma \mathbf{q}^2 W_2(\mathbf{q}) - \lambda \mathbf{q}^2], \quad (23a)$$

$$\begin{aligned} \partial_t W_3(\mathbf{q}_1, \mathbf{q}_2, \mathbf{q}_3) &= -3 [\gamma \mathbf{q}_1^2 W_3(\mathbf{q}_2, \mathbf{q}_3) + \gamma' \mathbf{q}_1^2 W_2(\mathbf{q}_2) W_2(\mathbf{q}_3) \\ &\quad + 2\lambda' \mathbf{q}_1 \cdot \mathbf{q}_2 W_2(\mathbf{q}_3)]_{123}, \end{aligned} \quad (23b)$$

$$\begin{aligned} \partial_t W_4(\mathbf{q}_1, \mathbf{q}_2, \mathbf{q}_3, \mathbf{q}_4) &= -4 [\gamma \mathbf{q}_1^2 W_4(\mathbf{q}_2, \mathbf{q}_3, \mathbf{q}_4) + 3\gamma' \mathbf{q}_1^2 W_2(\mathbf{q}_2) W_3(\mathbf{q}_3, \mathbf{q}_4) \\ &\quad + \gamma'' \mathbf{q}_1^2 W_2(\mathbf{q}_2) W_2(\mathbf{q}_3) W_2(\mathbf{q}_4) + 3\lambda' \mathbf{q}_1 \cdot \mathbf{q}_2 W_3(\mathbf{q}_3, \mathbf{q}_4) \\ &\quad + 3\lambda'' \mathbf{q}_1 \cdot \mathbf{q}_2 W_2(\mathbf{q}_3) W_2(\mathbf{q}_4)]_{1234}, \end{aligned} \quad (23c)$$

where $\gamma = \lambda\alpha'$ is the diffusion coefficient. In Eqs. (23), we suppressed arguments t and \mathbf{x} , as they are the same for all functions W_k . Furthermore, note that all arguments of each function W_k add up to zero — reminiscent of the momentum conservation in Feynman diagrams. Therefore, to save space, we omitted the first argument in W_k , where this argument can be inferred from the condition $\mathbf{q}_1 + \dots + \mathbf{q}_k = 0$. For example, $W_2(\mathbf{q}) \equiv W_2(\mathbf{q}) \equiv W_2(-\mathbf{q}, \mathbf{q})$ or $W_3(\mathbf{q}_3, \mathbf{q}_4) \equiv W_3(-\mathbf{q}_3 - \mathbf{q}_4, \mathbf{q}_3, \mathbf{q}_4)$. The symbol $[\dots]_{\overline{1\dots k}}$ denotes the sum over all permutations of $\mathbf{q}_1, \dots, \mathbf{q}_k$ divided by $1/k!$, *i.e.*, the average over all permutations. The diagrammatic representation of Eqs. (23) is given in Ref. [37] (see also Fig. 5).

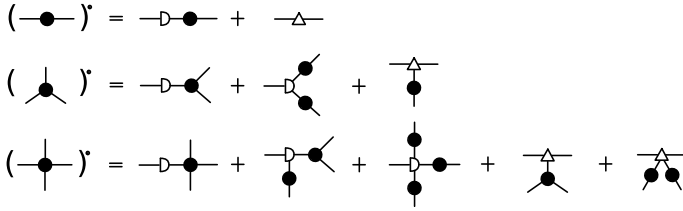


Fig. 5. Diagrammatic representation of Eqs. (23). See Refs. [37, 38].

Equations (23) represent the leading order in hydrodynamic gradient expansion. The next order would correspond to loop diagrams (in terms of the diagrammatic technique used in Fig. 5). It represents the feedback of fluctuations. For two-point functions, such feedback has been considered in Refs. [31–36], and the corresponding renormalization of hydrodynamic equations has been shown to remove cutoff dependence due to the “infinite noise” problem, as discussed above in Section 3.2.

3.5. Confluent formalism for arbitrary relativistic flow

For a *relativistic* fluid with non-trivial velocity gradients, the definition of the equal-time correlator in Eq. (18) and its Wigner transform are insufficient since the rest frame of the fluid is different at different space-time points, and the concept of “equal time” is thus ambiguous. To maintain the Lorentz covariance in the description of fluctuations, Ref. [35], and for non-Gaussian fluctuations, Ref. [38], propose to use averaged local rest frame of the fluid at the midpoint $x \equiv (t, \mathbf{x})$ of the correlator to define “equal time”. The same locally defined frame is also used to define, or measure, fluctuations of velocity.

The idea is to equip every space-time point x with an orthonormal triad of basis 4-vectors $e_{\hat{a}}(x)$, $\hat{a} = 1, 2, 3$, or $e(x)$, spatial in the local rest frame of the fluid at that point, *i.e.*,

$$e(x) \cdot u(x) = \mathbf{0}. \quad (24)$$

One can then define equal-time k -point correlators as functions of k space-time points expressed as

$$x_1 = x + \mathbf{e}(x) \cdot \mathbf{y}_1, \quad \dots, \quad x_k = x + \mathbf{e}(x) \cdot \mathbf{y}_k, \quad (25)$$

in terms of the midpoint x and the separation 3-vectors $\mathbf{y}_1, \dots, \mathbf{y}_k$, which sum to zero: $\mathbf{y}_1 + \dots + \mathbf{y}_k = 0$.

Some of the fields in the correlator may not be Lorentz scalars, for example, fluctuations of velocity, δu . One would like to express such fluctuations in a frame associated with the fluid, such as the local rest frame, rather than in an arbitrary lab frame. The local rest frame of the fluid is, however, different for different points x_1, \dots, x_k . To use the same frame for all points while making sure that fluctuations represent deviations from the fluid at rest locally, we boost the fluctuation variables (if they are not scalars) from the rest frame at the point they occur, say, at $x + \mathbf{y}_1$, to that at the midpoint x of the correlator. This operation leads to the *confluent correlator* defined as

$$H_{a_1 \dots a_k}(x_1, \dots, x_k) \equiv \left\langle [\Lambda(x, x_1) \delta \Psi(x_1)]_{a_1} \dots [\Lambda(x, x_k) \delta \Psi(x_k)]_{a_k} \right\rangle^c, \quad (26)$$

where $\Lambda(x, x_1)$ performs the boost on the corresponding fluctuation field $\delta \Psi(x_1)$ such that the 4-velocities in points x_1 and x are related by

$$\Lambda(x, x_1) u(x_1) = u(x). \quad (27)$$

Superscript “c” means “connected” as in Eq. (18).

We can now take the multipoint Wigner transform of the confluent correlator we just defined in Eq. (26) with respect to the 3-vectors $\mathbf{y}_1, \dots, \mathbf{y}_k$ describing the separation of the points in the local basis at point x (cf. Eq. (20))

$$\begin{aligned} W_{a_1 \dots a_k}(x; \mathbf{q}_1, \dots, \mathbf{q}_k) &\equiv \int d^3 \mathbf{y}_1 e^{-i \mathbf{q}_1 \cdot \mathbf{y}_1} \dots \int d^3 \mathbf{y}_k e^{-i \mathbf{q}_k \cdot \mathbf{y}_k} \\ &\times \delta^{(3)} \left(\frac{\mathbf{y}_1 + \dots + \mathbf{y}_k}{k} \right) H_{a_1 \dots a_k}(x + \mathbf{e}(x) \cdot \mathbf{y}_1, \dots, x + \mathbf{e}(x) \cdot \mathbf{y}_k). \end{aligned} \quad (28)$$

The inverse is given by (cf. Eq. (21))

$$\begin{aligned} &H_{a_1 \dots a_k}(x + \mathbf{e}_1(x) \cdot \mathbf{y}_1, \dots, x + \mathbf{e}_k(x) \cdot \mathbf{y}_k) \\ &= \int \frac{d^3 \mathbf{q}_1}{(2\pi)^3} e^{i \mathbf{q}_1 \cdot \mathbf{y}_1} \dots \int \frac{d^3 \mathbf{q}_k}{(2\pi)^3} e^{i \mathbf{q}_k \cdot \mathbf{y}_k} \\ &\times \delta^{(3)} \left(\frac{\mathbf{q}_1 + \dots + \mathbf{q}_k}{2\pi} \right) W_{a_1 \dots a_k}(x; \mathbf{q}_1, \dots, \mathbf{q}_k). \end{aligned} \quad (29)$$

Care must be taken also in defining a derivative with respect to the midpoint of such a correlation function in order to maintain the “equal-time in local rest frame” condition. The local rest frame is different in points x and $x + \Delta x$ used to define the derivative. A derivative which maintains the “equal-time” condition is introduced in Refs. [35, 36] and termed *confluent derivative*. It is defined via the $\Delta x \rightarrow 0$ limit of the following equation:

$$\begin{aligned} \Delta x \cdot \bar{\nabla} W_{a_1 \dots a_k}(x; \mathbf{q}_1, \dots, \mathbf{q}_k) &\equiv \Lambda(x, x + \Delta x)_{a_1}^{b_1} \dots \Lambda(x, x + \Delta x)_{a_k}^{b_k} \\ &\times W_{b_1 \dots b_k}(x; \mathbf{q}'_1, \dots, \mathbf{q}'_k) - W_{a_1 \dots a_k}(x; \mathbf{q}_1, \dots, \mathbf{q}_k), \end{aligned} \quad (30)$$

where

$$\mathbf{q}' = \mathbf{e}(x + \Delta x) \cdot [\Lambda(x + \Delta x, x) \mathbf{e}(x) \cdot \mathbf{q}] \equiv R(x + \Delta x, x) \mathbf{q}. \quad (31)$$

In Eq. (30), the (non-scalar) fluctuation fields are boosted from point $x + \Delta x$ back to point x , similar to the definition of the confluent correlator in Eq. (26). In addition, at $x + \Delta x$, we evaluate the function using the set of 3-wave-vectors \mathbf{q}'_i given by Eq. (31), different from the set \mathbf{q}_i used at point x . The new set is obtained by representing each vector \mathbf{q} as a 4-vector orthogonal to $u(x)$, $\mathbf{e}(x) \cdot \mathbf{q}$, then boosting this vector to the rest frame at point $x + \Delta x$, and then expressing it again as a 3-vector, but now in the basis $\mathbf{e}(x + \Delta x)$ orthogonal to $u(x + \Delta x)$. The resulting transformation of vector \mathbf{q} is a rotation, denoted by R in Eq. (31).

Taking the limit $\Delta x \rightarrow 0$ in Eq. (30), one can express confluent derivative as follows:

$$\bar{\nabla}_\mu W_{a_1 \dots a_2} = \partial_\mu W_{a_1 \dots a_2} + k \left(\bar{\omega}_{\mu b}^{\dot{a}} q_{1\dot{a}} \frac{\partial}{\partial q_{1b}} W_{a_1 \dots a_k} - \bar{\omega}_{\mu a_1}^b W_{ba_2 \dots a_k} \right)_{\overline{1 \dots k}}, \quad (32)$$

where the confluent connection $\bar{\omega}$ is a generator of the infinitesimal boost Λ and $\dot{\omega}$ is a generator of the infinitesimal rotation R

$$\Lambda(x + \Delta x, x)_{\dot{b}}^a = \delta_b^a - \Delta x^\mu \bar{\omega}_{\mu b}^a, \quad (33)$$

$$R(x + \Delta x, x)_{\dot{b}}^{\dot{a}} = \delta_{\dot{b}}^{\dot{a}} - \Delta x^\mu \dot{\omega}_{\mu b}^{\dot{a}}. \quad (34)$$

The indices $a, b, a_1 \dots a_k$ label fluctuating fields. The confluent connection $\bar{\omega}_{\mu b}^a$ is non-zero when indices a, b refer to different components of a Lorentz vector (such as δu). In this case, the connection satisfies

$$\bar{\nabla}_\mu u^\alpha \equiv \partial_\mu u^\alpha + \bar{\omega}_{\mu\beta}^\alpha u^\beta = 0, \quad (35)$$

(local velocity is “confluently” constant), which follows from Eqs. (27) and (33)⁴.

⁴ For a scalar field (*e.g.*, energy density, pressure fluctuations, *etc.*), the confluent connection is, of course, zero. *E.g.*, $\bar{\nabla}_\mu \delta m = \partial_\mu \delta m$.

The rotation connection $\bar{\omega}$ is determined by Eqs. (31) and (34)

$$\bar{\omega}_{\mu\hat{a}}^{\hat{b}} = e_{\alpha}^{\hat{b}} \left(\partial_{\mu} e_{\hat{a}}^{\alpha} + \bar{\omega}_{\mu\beta}^{\alpha} e_{\hat{a}}^{\beta} \right). \quad (36)$$

Naturally, it satisfies

$$\bar{\nabla}_{\mu} e_{\hat{a}}^{\alpha} \equiv \partial_{\mu} e_{\hat{a}}^{\alpha} + \bar{\omega}_{\mu\beta}^{\alpha} e_{\hat{a}}^{\beta} - \bar{\omega}_{\mu\hat{a}}^{\hat{b}} e_{\hat{b}}^{\alpha} = 0 \quad (37)$$

(local basis vectors are confluent constant).

The boost A is not defined uniquely by Eq. (27) — only up to a rotation keeping u unchanged. The simplest choice is the boost without additional rotation, which corresponds to confluent connection given explicitly by

$$\bar{\omega}_{\mu\beta}^{\alpha} = u_{\beta} \partial_{\mu} u^{\alpha} - u^{\alpha} \partial_{\mu} u_{\beta}. \quad (38)$$

For this choice of the confluent connection, the rotation connection also simplifies to

$$\bar{\omega}_{\mu\hat{a}}^{\hat{b}} = e_{\alpha}^{\hat{b}} \partial_{\mu} e_{\hat{a}}^{\alpha}. \quad (39)$$

3.6. Evolution equations for hydrodynamic fluctuations

There are five normal hydrodynamics modes, which can be described as two propagating modes and three diffusive⁵. The propagating modes correspond to fluctuations of pressure mixed with the fluctuations of the longitudinal (with respect to the wave-vector \mathbf{q}) velocity. The frequency of these sound modes is $c_s|\mathbf{q}|$. The diffusive modes are the fluctuations of the specific entropy $m \equiv s/n$ at fixed pressure and transverse velocity. The relaxation rate of these modes is proportional to the square of their wave-number \mathbf{q}^2 . The slowest diffusive mode near the critical point is specific entropy because its diffusion constant vanishes at the critical point.

In this review, we shall focus on the slowest diffusive mode m for two reasons. First, because it is the slowest and, therefore, the furthest from equilibrium mode. Second, in equilibrium, this mode shows the fluctuations of the order parameter (*i.e.*, $\delta m \sim \delta\phi$, Eq. (4)), divergent at the critical point.

The evolution equation for the Wigner-transformed confluent two-point correlator of the specific entropy fluctuations, $\langle \delta m \delta m \rangle$, derived in Ref. [36] reads

$$\mathcal{L}[W_{mm}(\mathbf{q})] = (\partial \cdot u) W_{mm}(\mathbf{q}) - 2\gamma_{mm} \mathbf{q}^2 \left[W_{mm}(\mathbf{q}) - \frac{c_p}{n^2} \right], \quad (40)$$

⁵ We focus on hydrodynamics involving baryon charge. Each additional charge adds one diffusive mode to the count.

where $\gamma_{mm} \equiv \kappa/c_p$ — the heat diffusion constant, and \mathcal{L} is the Liouville operator given by

$$\mathcal{L}[W_{mm}] \equiv \left[u \cdot \bar{\nabla} - \partial_\nu u^\mu (e_\mu \cdot \mathbf{q}) \left(e^\nu \cdot \frac{\partial}{\partial \mathbf{q}} \right) \right] W_{mm}. \quad (41)$$

The first term is the confluent derivative along the flow of the fluid, while the second describes stretching and/or rotation of the vectors \mathbf{q} due to the expansion and/or rotation of the fluid. In the case of expansion, one can think of this term as describing the Hubble-like “red shift” of the fluctuation wave-vector \mathbf{q} . For example, for Bjorken flow the Liouville operator takes the form

$$\mathcal{L}_{\text{Bj}} = \partial_\tau - \frac{q_3}{\tau} \frac{\partial}{\partial q_3}, \quad (42)$$

where the second term describes the “stretching” of the fluctuations, *i.e.*, the “red shift” of the wave-number q_3 due to longitudinal expansion⁶.

The first term on the r.h.s. of Eq. (40) describes the scaling of the fluctuation magnitude with the volume of a hydrodynamic cell, as the cell expands at the rate $\partial \cdot u$. This trivial rescaling could be absorbed by multiplying W by a conserved density, such as the baryon density, n . The equation for a rescaled function $N_{mm} \equiv nW_{mm}$ is the same as in Eq. (40), but without the $\partial \cdot u$ term

$$\mathcal{L}[N_{mm}(\mathbf{q})] = -2\gamma_{mm}\mathbf{q}^2 \left[N_{mm}(\mathbf{q}) - \frac{c_p}{n} \right]. \quad (43)$$

The last term in Eq. (40) describes the diffusive relaxation of fluctuations towards equilibrium given by thermodynamic quantity c_p/n^2 (or c_p/n for N_{mm}).

It is instructive to compare Eq. (40) for W_{mm} (or the corresponding Eq. (43) for N_{mm}) to Eq. (23a) for the density–density correlator $\langle \delta n \delta n \rangle$ in the diffusion problem. The main difference is that the time derivative is replaced by the Liouville operator, which takes into account the flow of the fluid. The $(\partial \cdot u)$ term on the r.h.s. (absent when Eq. (40) is written in terms of N_{mm} , Eq. (43)) is also an effect of the flow — expansion. The diffusive relaxation terms are different because the correlated quantities are different, $\delta m \delta m$ in Eq. (40) and $\delta n \delta n$ in Eq. (23a). The coefficients, however, can be mapped onto each other via substitution

$$n \rightarrow m, \quad \gamma = \lambda \alpha' \rightarrow \gamma_{mm} = \frac{\kappa}{c_p}, \quad \lambda \rightarrow \frac{\kappa}{n}, \quad W_2 \rightarrow N_{mm}. \quad (44)$$

⁶ Naturally, we have chosen the triad of the 4 vectors \mathbf{e} in such a way that the spatial part of the 4-vector e_3 points along the direction of the longitudinal flow, while the e_1 and e_2 are constant. In this case, the rotation connection ($\tilde{\omega}$) terms vanish in the confluent derivative in Eq. (32). The confluent connection ($\tilde{\omega}$) terms are absent already for arbitrary flow because the fluctuating quantity, m , is a scalar.

The evolution equations for non-Gaussian correlators W_{mmm} and W_{mmmm} (or $N_{mmm} \equiv n^2 W_{mmm}$ and $N_{mmmm} \equiv n^3 W_{mmmm}$) are qualitatively similar to those in the diffusion problem in Eq. (23b) and (23c). However, unlike the case of W_{mm} , where the whole equation (43) can be obtained from Eq. (23a) for W_2 by the substitution given by Eq. (44), only the terms containing leading singularities at the critical point can be obtained from Eq. (23b) and (23c) by the substitution (44) (with $W_3 \rightarrow N_{mmm}$ and $W_4 \rightarrow N_{mmmm}$). There are subleading singularities, which are due to the non-linearity of the mapping $n \rightarrow m$. These terms are written explicitly in Ref. [38].

4. Freeze-out of fluctuations and observables

The previous section was devoted to recent progress in describing the evolution of fluctuations in hydrodynamics using correlators of hydrodynamic variables in *coordinate* space. Heavy-ion collision experiments do not measure such densities, or their correlations, directly. Instead, the particle multiplicities and their correlations in *momentum* space are measured. In this section, we describe how to connect the theoretical description in terms of fluctuating hydrodynamics to these experimental observables.

4.1. Event-by-event fluctuations and their experimental measures

Typical experimental measures are cumulants of the event-by-event fluctuations or correlations of particle multiplicities. For example, if N_p is the proton number in an event, its fluctuation in the event is $\delta N_p \equiv N_p - \langle N_p \rangle$ and $\langle (\delta N)^2 \rangle$ is its quadratic cumulant, or variance, where $\langle \dots \rangle$ is the event average. Higher-order cumulants, measuring non-Gaussianity of fluctuations, are constructed similarly (see, *e.g.*, Ref. [8] for a review).

In addition, correlations between particles can be also measured, such as $\langle \delta N_p \delta N_\pi \rangle$ — a correlation between proton and pion multiplicities. Such measures can also include higher-order correlators [40]. Similarly to correlations between species, one can also consider correlations between particles with different momenta.

The number of particles $d^3 N_i$ in a given momentum cell $d^3 p$ is given by the well-known Cooper–Frye formula [41]

$$d^3 N_i = \frac{d^3 p}{(2\pi)^3} \frac{p^\mu}{p^0} \int_{\Sigma} d^3 \Sigma_\mu(x) f_i(x, p) \quad (45)$$

in terms of the phase-space distribution function $f_i(x, p)$ integrated over the freeze-out hypersurface Σ . Therefore, the correlations between different momentum cells and/or between different species can be expressed in terms of the correlation functions of fluctuations of $f_i(x, p)$: $\delta f \equiv f - \langle f \rangle$.

To simplify and shorten notations, we shall combine the species index (which includes all discrete quantum numbers, such as mass, spin, isospin, *etc.*) together with the coordinate and momentum into a single composite index $A = \{i, x, p\}$. Therefore, the general correlator which, upon integration over the freeze-out hypersurface, gives the observable correlation measures has the form

$$\langle \delta f_{i_1}(x_1, p_1) \dots \delta f_{i_k}(x_k, p_k) \rangle \equiv \langle \delta f_{A_1} \dots \delta f_{A_k} \rangle. \quad (46)$$

Usually, the Cooper–Frye prescription (45) is applied to determine the event-by-event *averaged* number of particles in terms of the averaged distribution function $\langle f_A \rangle$. This averaged function is expressed in terms of the hydrodynamic variables, or fields, $T(x)$ and $\mu(x)$

$$\langle f_A \rangle \equiv \langle f_{i_A}(x_A, p_A) \rangle = [\exp \{ \beta(x) u(x) \cdot p_A - \alpha(x) q_A \} - (-1)^{2s_A}]^{-1}, \quad (47)$$

where $\beta = 1/T$, $\alpha = \mu/T$, q_A is the charge of the particle A with respect to the chemical potential μ (baryon charge, for example), and s_A is the spin of the particle.

In order to convert hydrodynamic *fluctuations* into particle event-by-event fluctuations, we need an analogous freeze-out prescription for *correlators* in Eq. (46).

4.2. Freeze-out of fluctuations and the maximum entropy method

The generalization of the Cooper–Frye freeze-out to fluctuations has been first considered in Ref. [16]. In the approach of Ref. [16], the fluctuations of the phase-space distribution function $f(x, p)$ are assumed to be caused by fluctuations of the hydrodynamic variables/fields $T(x)$ and $\mu(x)$ on which $f(x, p)$ depends, as in Eq. (47). As a result, coordinate space correlations in $T(x)$ and $\mu(x)$ translate into the phase-space correlations in $f(x, p)$.

This approach has an important flaw, which becomes obvious if one considers fluctuations in an (almost) ideal gas. In this case, there are fluctuations of hydrodynamic variables, such as charge density $n(x)$, but there are no momentum space correlations of $f(x, p)$, which would, nevertheless, be produced if the approach of Ref. [16] were to be applied. Instead, the hydrodynamic fluctuations of $n(x)$ are matched on the particle side by trivial (Poisson, in the ideal gas case) *uncorrelated* fluctuations of the occupation numbers in each phase-space point.

This problem has been addressed in Refs. [42, 43] by subtracting this trivial ideal gas contribution from hydrodynamic fluctuations of $n(x)$ before applying the procedure of Ref. [16] to the remainder, which is due to interactions and out-of-equilibrium dynamics.

Generalization of this approach to fluctuations of other hydrodynamic variables, and to non-Gaussian fluctuations, proved elusive until the principle of maximum entropy for fluctuations was proposed and implemented in Ref. [23]. In this approach, the matching of conserved hydrodynamic densities such as $\epsilon(x)$ and $\tilde{n}_q(x)$, defined in Eqs. (10) and (11), is done on an event-by-event basis. For example, we have to match the fluctuations of conserved charge density

$$\delta n_q(x) = \sum_i \int_p q_i \delta f_i(x, p) \equiv \int_{\tilde{A}} q_A \delta f_A(x) \equiv \int_A q_A \delta^{(3)}(x - x_A) \delta f_A, \quad (48)$$

where \int_p is a 3-integral over momenta with the Lorentz-invariant measure and \sum_i is a sum over the species of particles with id label i (corresponding to mass, spin, isospin, *etc.*) carrying charge q_i corresponding to density n_q (*e.g.*, baryon charge when $n_q = n_B$ is the baryon density). We have also introduced a convenient shorthand $\int_{\tilde{A}}$, which denotes the sum and the momentum space integral together (but no space integration). One can think of the composite index A as describing not only the particle “id” (*i.e.*, mass, spin, *etc.*) but also its position in the phase space (as if each particle species has its own phase space): $A \equiv \{i_A, p_A, x_A\}$. Finally, we also introduced \int_A , which includes integration over the whole phase space (momentum p_A and coordinate x_A) of each particle species, and a convenient shorthand $f_A \equiv f_A(x_A)$. The delta function simply reflects the locality of freeze-out (*i.e.*, each hydrodynamic cell at point x is converted into particles located at the same position $x_A = x$). Similarly, matching of the energy-momentum density requires

$$\delta(\epsilon(x)u^\mu(x)) = \int_{\tilde{A}} p^\mu \delta f_A(x) \equiv \int_A p^\mu \delta^{(3)}(x - x_A) \delta f_A. \quad (49)$$

It is convenient to organize equations such as (48) and (49) into an indexed array, where lowercase index a runs through five hydrodynamic variables $\delta\Psi_a = \delta\{n_q, \epsilon u^\mu\}$, similar to Eq. (11)

$$\delta\Psi_a \equiv \delta\Psi_a(x_a) = \int_A P_a^A \delta f_A, \quad (50)$$

where

$$P_a^A = \{q_A, p_A^\mu\} \delta^{(3)}(x_a - x_A) \quad (51)$$

is the array of the contributions of a single particle at point x_A to hydrodynamic densities $\Psi_a = \{n, \epsilon u^\mu\}$ in a cell around point x_a on the freeze-out

surface. Similarly to particle index A , it is convenient to view hydrodynamic field index a as a composite index labeling both the field and the point on the freeze-out surface where the value of this field is measured.

Equation (50) for fluctuations imply relationships between the hydrodynamic correlators in space points $x_{a_1} \dots x_{a_k}$,

$$H_{a_1 \dots a_k} \equiv \langle \delta \Psi_{a_1} \dots \delta \Psi_{a_k} \rangle, \quad (52)$$

and particle correlators in phase-space points $A_1 \dots A_k$,

$$G_{A_1 \dots A_k} \equiv \langle \delta f_{A_1} \dots \delta f_{A_k} \rangle, \quad (53)$$

which have the form

$$H_{a_1 \dots a_k} = \int_{A_1 \dots A_k} G_{A_1 \dots A_k} P_{a_1}^{A_1} \dots P_{a_k}^{A_k}. \quad (54)$$

Equations (54) represent constraints on the particle correlators $G_{AB\dots}$ imposed by conservation laws. These constraints alone are not enough to completely determine $G_{AB\dots}$ simply because there are more “unknowns” $G_{AB\dots}$ than the constraints. The situation is similar already for ensemble (*i.e.*, event) averaged quantities, or one-point functions. In this case, the knowledge of the averaged energy, momentum, and baryon density is not sufficient alone to determine the particle distribution functions f_A . Additional input is needed.

In the absence of additional information, the most natural solution is the one which maximizes the entropy of the resonance gas into which the hydrodynamically evolved fireball freezes out. That entropy is given by the functional of f_A

$$S[f_A] = \int_A (\theta_A^{-1} + f_A) \ln(1 + \theta_A f_A) - f_A \ln f_A, \quad (55)$$

where $\theta_A = (-1)^{2s_A}$ is determined by the particle spin s_A ⁷. Maximizing $S[f_A]$, subject to the constraints on f_A imposed by conservation laws, produces the well-known equilibrium distribution f_A given in Eq. (47), underlying the Cooper–Frye freeze-out procedure, which has been widely and successfully used for describing experimental data for half a century. This observation has been also used recently to describe systematically deviations from equilibrium due to viscous or diffusive gradients in Ref. [44].

⁷ Neglecting quantum statistics, *i.e.*, taking $\theta_A \rightarrow 0$, one obtains the familiar Boltzmann entropy $S[f_A] = \int_A f_A (1 - \ln f_A)$.

In order to apply the maximum entropy approach to *fluctuation* freeze-out, one needs the entropy of fluctuations as a functional of f_A as well as correlators G_{AB} , G_{ABC} , *etc.* Conceptually, this entropy, $S[f_A, G_{AB}, \dots]$ represents the (logarithm) of the number of the microscopic states in the resonance gas ensemble with the given set of correlators. The single-particle entropy $S[f_A]$ is the value of $S[f_A, G_{AB}, \dots]$ when all correlators $G_{AB\dots}$ are given by their values in the equilibrium resonance gas.

The expression for the functional $S[f_A, G_{AB}, \dots]$ was found in Ref. [23]. For example, keeping only terms with the out-of-equilibrium two-point correlators it reads⁸

$$S_2[f, G] = S[f] + \frac{1}{2} \text{Tr} [\log(CG) - CG + 1] . \quad (56)$$

The last term is always negative except for $G = C^{-1} \equiv \bar{G}$ which is the equilibrium value of the correlator G , where $C_{AB} = -\delta^2 S[f]/(\delta f_A \delta f_B)$. When $G = \bar{G}$, the last term vanishes and S_2 is maximized with respect to G .

However, maximizing the entropy in Eq. (56) with respect to G under constraints in Eq. (54) gives

$$(G^{-1})^{AB} = (\bar{G}^{-1})^{AB} + (H^{-1} - \bar{H}^{-1})^{ab} P_a^A P_b^B . \quad (57)$$

In this equation and below, the repeated lowercase indices a, b , *etc.* imply summation over the set hydrodynamic variables Ψ_a, Ψ_b , and volume integration over hydrodynamic cells at points x_a, x_b . Due to the delta functions in the definition of P_a^A in Eq. (51), these implied integrals in Eq. (57) simply set the spatial arguments of $(G^{-1})^{AB}$ to those of $(H^{-1})^{ab}$, *i.e.*, $x_A = x_a$ and $x_B = x_b$. When hydrodynamic correlator H equals its equilibrium value \bar{H} in the resonance gas, the particle correlator G equals \bar{G} — its value in the resonance gas (*i.e.*, $f_A \delta_{AB}$, neglecting quantum statistics).

If deviations of fluctuations from equilibrium resonance gas are small, equation (57) can be linearized in such deviations. The deviations could be due to non-equilibrium effects, which have to be small for hydrodynamics to apply, or due to effects of the critical point. The linearized equation relates deviations of the particle correlators $\Delta G_{AB} = G_{AB} - \bar{G}_{AB}$ to the deviations of the hydrodynamics correlators $\Delta H_{ab} = H_{ab} - \bar{H}_{ab}$ from the resonance gas values

$$\Delta G_{AB} = \Delta H_{ab} (\bar{H}^{-1} P \bar{G})_A^a (\bar{H}^{-1} P \bar{G})_B^b . \quad (58)$$

Similarly, the non-Gaussian cumulants $G_{ABC\dots}$ of particle fluctuations can be expressed in terms of the non-Gaussian cumulants of the hydrodynamic variables $H_{abc\dots}$. Such non-linear relations similar to Eq. (57) can be derived from the corresponding entropy functional found in Ref. [23] and we will not reproduce them here.

⁸ The calculation of the entropy of fluctuations along these lines for a two-point correlator of *hydrodynamic* variables can be found in Ref. [34], and it is *mathematically* similar to the 2-PI action in quantum field theory [45–49].

Linearized relations valid for small deviations from the equilibrium resonance gas, however, are simple and instructive. The relationship is similar to Eq. (58), but instead of the “raw” deviations from equilibrium $\Delta G_{AB\dots}$ and $\Delta H_{ab\dots}$, *i.e.* correlations relative to equilibrium, the proportionality relation holds between *irreducible* relative correlators $\hat{\Delta}G_{AB\dots}$ defined in Ref. [23]. An irreducible correlator $\hat{\Delta}G$ is different from the “raw”, or reducible, relative correlator ΔG by subtraction of correlations involving only a smaller subset of the points $AB\dots$. The irreducible ΔH differs from ΔH similarly. The resulting linear relation generalizes Eq. (58)

$$\hat{\Delta}G_{A_1\dots A_k} = \hat{\Delta}H_{a_1\dots a_k} (\bar{H}^{-1}P\bar{G})_{A_1}^{a_1} \dots (\bar{H}^{-1}P\bar{G})_{A_k}^{a_k}, \quad (59)$$

where $\hat{\Delta}G$ and $\hat{\Delta}H$ denote *irreducible* relative correlators for particles and for hydrodynamic variables, respectively. For two-point (Gaussian) correlators $\hat{\Delta}G = \Delta G$ and $\hat{\Delta}H = \Delta H$ and Eq. (57) reproduces Eq. (57).

Equation (58) thus solves the problem of translating fluctuations in hydrodynamics into correlations between particles at freeze-out, in such a way as to obey the conservation laws on an event-by-event basis (by satisfying constraints in Eq. (54)). As one can see, it systematically eliminates spurious “self-correlations” discussed at the beginning of this section not only for Gaussian, but also for non-Gaussian cumulants.

Similarly to the way the maximum entropy approach reproduces and generalizes the Cooper–Frye prescription for event *averaged* observables, the maximum entropy approach to fluctuations reproduces, justifies, and generalizes prior approaches to freezing out fluctuations, in particular, of critical fluctuations, as shown in Ref. [23]. Such a prior approach involving fluctuating background field σ was introduced in Ref. [15], generalized to non-Gaussian fluctuations in Refs. [20, 40], and then further generalized to *non-equilibrium* fluctuations in Ref. [50].

The σ -field approach [15, 20, 40], however, besides the knowledge of QCD EoS, requires the knowledge of the properties of the field σ such as its correlation length as well as its coupling to observed particles. These properties would depend on the nature of this field — an *a priori* unknown mixture of scalar fields such as chiral condensate, energy, and baryon number densities. It was also not clear how to deal with non-critical fluctuations or contributions of lower-point correlations to higher-point correlators. All these uncertainties are absent in the maximum entropy approach. The correlations described by Eq. (59) are very similar to the correlations induced by the σ field given by a mixture of hydrodynamic fields determined by the QCD EoS itself.

The maximum entropy approach thus provides a direct connection between the fluctuations of the hydrodynamic quantities and the observed particle multiplicities, with their fluctuations. This connection is determined by the EoS of QCD in the resonance gas phase where the freeze-out occurs. The effects of the critical point and non-equilibrium are encoded in the non-trivial correlations described quantitatively by Eq. (59).

5. Summary and conclusions

These lecture notes describe recent theory developments aimed at mapping QCD phase diagram and the search for the critical point in heavy-ion collisions.

The existence and location of the QCD critical point is a major unanswered question about the QCD phase diagram. Universality of critical phenomena allows us to draw predictions which do not require precise microscopic knowledge of QCD dynamics.

In particular, singular behavior of the fluctuations at critical points should manifest itself in non-monotonic dependence of the fluctuation measures in heavy-ion collisions as the critical point is approached and then passed in the course of the beam-energy scan. This dependence is especially pronounced for non-Gaussian fluctuation measures.

The dynamical nature of the heavy-ion collision fireball requires treatment of fluctuations *beyond equilibrium* thermodynamics. This means not only that we need to be able to describe fluctuations of hydrodynamic variables, but also that we need to be able to translate those hydrodynamic fluctuations into the fluctuations and correlations of particle multiplicities observable in experiments. The understanding of how to do this in a way consistent with hydrodynamics, in particular, with conservation laws, has only emerged recently. These recent developments are the focus of the lectures.

As is often the case with a developing field of research, these lectures can only attempt to capture a snapshot of the current state of the art. Some questions still require more careful analyses, and some tools, such as fully-fledged simulation of the heavy-ion collision with fluctuations, still need to be developed before comparison to experiment can become quantitative and reliable. Naturally, much of the future development of the field will be informed by the experimental data from the BES-II program at RHIC as well as from experiments at planned future heavy-ion collision facilities [51].

I would like to express my gratitude to the organizers of the 63rd Cracow School of Theoretical Physics for their warm hospitality in Zakopane. This work is supported by the U.S. Department of Energy, Office of Science, Office of Nuclear Physics Award No. DE-FG0201ER41195.

REFERENCES

- [1] C. Cagniard de la Tour, «On the effect of heat and compression», *Ann. Phil. New Ser.* **5**, 290 (1823).
- [2] Y. Goudaroulis, «Searching for a name: the development of the concept of the critical point (1822–1869)», *Rev. Hist. Sci.* **47**, 353 (1994).
- [3] T. Andrews, «XVIII. *The Bakerian Lecture* — On the continuity of the gaseous and liquid states of matter», *Phil. Trans. Roy. Soc.* **159**, 575 (1869).
- [4] J. van der Waals, «Over de Continuïteit van den Gas en Vloeistofoestand», Ph.D. Thesis, Leiden Univ., 1873.
- [5] M. v. Smoluchowski, «Molekular-kinetische Theorie der Opaleszenz von Gasen im kritischen Zustande, sowie einiger verwandter Erscheinungen», *Ann. Phys.* **330**, 205 (1908).
- [6] A. Einstein, «Theorie der Opaleszenz von homogenen Flüssigkeiten und Flüssigkeitsgemischen in der Nähe des kritischen Zustandes», *Ann. Phys.* **338**, 1275 (1910).
- [7] L.D. Landau, «On the Theory of Phase Transitions», *Zh. Eksp. Teor. Fiz.* **7**, 19 (1937).
- [8] A. Bzdak *et al.*, «Mapping the phases of quantum chromodynamics with beam energy scan», *Phys. Rep.* **853**, 1 (2020), [arXiv:1906.00936 \[nucl-th\]](#).
- [9] W. Zajc, «The Fluid Nature of Quark–Gluon Plasma», *Nucl. Phys. A* **805**, 283c (2008).
- [10] Y. Aoki *et al.*, «The order of the quantum chromodynamics transition predicted by the standard model of particle physics», *Nature* **443**, 675 (2006), [arXiv:hep-lat/0611014](#).
- [11] STAR Collaboration (M.M. Aggarwal *et al.*), «An Experimental Exploration of the QCD Phase Diagram: The Search for the Critical Point and the Onset of De-confinement», [arXiv:1007.2613 \[nucl-ex\]](#).
- [12] M.A. Stephanov, K. Rajagopal, E.V. Shuryak, «Signatures of the Tricritical Point in QCD», *Phys. Rev. Lett.* **81**, 4816 (1998), [arXiv:hep-ph/9806219](#).
- [13] M.A. Stephanov, «QCD Phase Diagram and the Critical Point», *Prog. Theor. Phys. Suppl.* **153**, 139 (2004), [arXiv:hep-ph/0402115](#).
- [14] L. Landau, E. Lifshitz, «Statistical Physics: Volume 5», *Elsevier Science*, 2013.
- [15] M.A. Stephanov, K. Rajagopal, E.V. Shuryak, «Event-by-event fluctuations in heavy ion collisions and the QCD critical point», *Phys. Rev. D* **60**, 114028 (1999), [arXiv:hep-ph/9903292](#).
- [16] J.I. Kapusta, B. Müller, M. Stephanov, «Relativistic theory of hydrodynamic fluctuations with applications to heavy-ion collisions», *Phys. Rev. C* **85**, 054906 (2012), [arXiv:1112.6405 \[nucl-th\]](#).
- [17] M.A. Stephanov, «Non-Gaussian Fluctuations near the QCD Critical Point», *Phys. Rev. Lett.* **102**, 032301 (2009), [arXiv:0809.3450 \[hep-ph\]](#).

- [18] D.J. Amit, «Field Theory, the Renormalization Group, and Critical Phenomena», *Singapore, World Scientific*, 1984.
- [19] A. Pelissetto, E. Vicari, «Critical phenomena and renormalization-group theory», *Phys. Rep.* **368**, 549 (2002), [arXiv:cond-mat/0012164](#).
- [20] M.A. Stephanov, «Sign of Kurtosis near the QCD Critical Point», *Phys. Rev. Lett.* **107**, 052301 (2011), [arXiv:1104.1627 \[hep-ph\]](#).
- [21] J.J. Rehr, N.D. Mermin, «Revised Scaling Equation of State at the Liquid–Vapor Critical Point», *Phys. Rev. A* **8**, 472 (1973).
- [22] J.F. Nicoll, «Critical phenomena of fluids: Asymmetric Landau–Ginzburg–Wilson model», *Phys. Rev. A* **24**, 2203 (1981).
- [23] M.S. Pradeep, M. Stephanov, «Maximum Entropy Freeze-Out of Hydrodynamic Fluctuations», *Phys. Rev. Lett.* **130**, 162301 (2023), [arXiv:2211.09142 \[hep-ph\]](#).
- [24] P. Parotto *et al.*, «QCD equation of state matched to lattice data and exhibiting a critical point singularity», *Phys. Rev. C* **101**, 034901 (2020), [arXiv:1805.05249 \[hep-ph\]](#).
- [25] STAR Collaboration (J. Adam *et al.*), «Nonmonotonic Energy Dependence of Net-Proton Number Fluctuations», *Phys. Rev. Lett.* **126**, 092301 (2021), [arXiv:2001.02852 \[nucl-ex\]](#).
- [26] STAR Collaboration (M.S. Abdallah *et al.*), «Cumulants and correlation functions of net-proton, proton, and antiproton multiplicity distributions in Au+Au collisions at energies available at the BNL Relativistic Heavy Ion Collider», *Phys. Rev. C* **104**, 024902 (2021), [arXiv:2101.12413 \[nucl-ex\]](#).
- [27] STAR Collaboration (M.S. Abdallah *et al.*), «Measurements of Proton High Order Cumulants in $\sqrt{s_{NN}} = 3$ GeV Au+Au Collisions and Implications for the QCD Critical Point», *Phys. Rev. Lett.* **128**, 202303 (2022), [arXiv:2112.00240 \[nucl-ex\]](#).
- [28] L. Landau, E. Lifshitz, «Statistical Physics, Part 2, vol. 9 of *Course of Theoretical Physics*», *Elsevier Science*, 2013.
- [29] M. Singh *et al.*, «Hydrodynamic Fluctuations in Relativistic Heavy-Ion Collisions», *Nucl. Phys. A* **982**, 319 (2019), [arXiv:1807.05451 \[nucl-th\]](#).
- [30] C. Chattopadhyay, J. Ott, T. Schaefer, V. Skokov, «Dynamic scaling of order parameter fluctuations in model B», *Phys. Rev. D* **108**, 074004 (2023), [arXiv:2304.07279 \[nucl-th\]](#).
- [31] Y. Akamatsu, A. Mazeliauskas, D. Teaney, «Kinetic regime of hydrodynamic fluctuations and long time tails for a Bjorken expansion», *Phys. Rev. C* **95**, 014909 (2017).
- [32] Y. Akamatsu, A. Mazeliauskas, D. Teaney, «Bulk viscosity from hydrodynamic fluctuations with relativistic hydrokinetic theory», *Phys. Rev. C* **97**, 024902 (2018).
- [33] M. Martinez, T. Schäfer, «Stochastic hydrodynamics and long time tails of an expanding conformal charged fluid», *Phys. Rev. C* **99**, 054902 (2019), [arXiv:1812.05279 \[hep-th\]](#).

- [34] M. Stephanov, Y. Yin, «Hydrodynamics with parametric slowing down and fluctuations near the critical point», *Phys. Rev. D* **98**, 036006 (2018), [arXiv:1712.10305 \[nucl-th\]](#).
- [35] X. An, G. Başar, M. Stephanov, H.-U. Yee, «Relativistic hydrodynamic fluctuations», *Phys. Rev. C* **100**, 024910 (2019), [arXiv:1902.09517 \[hep-th\]](#).
- [36] X. An, G. Başar, M. Stephanov, H.-U. Yee, «Fluctuation dynamics in a relativistic fluid with a critical point», *Phys. Rev. C* **102**, 034901 (2020), [arXiv:1912.13456 \[hep-th\]](#).
- [37] X. An, G. Başar, M. Stephanov, H.-U. Yee, «Evolution of Non-Gaussian Hydrodynamic Fluctuations», *Phys. Rev. Lett.* **127**, 072301 (2021), [arXiv:2009.10742 \[hep-th\]](#).
- [38] X. An, G. Başar, M. Stephanov, H.-U. Yee, «Non-Gaussian fluctuation dynamics in relativistic fluids», *Phys. Rev. C* **108**, 034910 (2023), [arXiv:2212.14029 \[hep-th\]](#).
- [39] A. Onuki, «Phase Transition Dynamics», *Cambridge University Press*, 2002.
- [40] C. Athanasiou, K. Rajagopal, M. Stephanov, «Using higher moments of fluctuations and their ratios in the search for the QCD critical point», *Phys. Rev. D* **82**, 074008 (2010), [arXiv:1006.4636 \[hep-th\]](#).
- [41] F. Cooper, G. Frye, «Single-particle distribution in the hydrodynamic and statistical thermodynamic models of multiparticle production», *Phys. Rev. D* **10**, 186 (1974).
- [42] B. Ling, T. Springer, M. Stephanov, «Hydrodynamics of charge fluctuations and balance functions», *Phys. Rev. C* **89**, 064901 (2014), [arXiv:1310.6036 \[nucl-th\]](#).
- [43] J.I. Kapusta, C. Plumberg, «Causal electric charge diffusion and balance functions in relativistic heavy-ion collisions», *Phys. Rev. C* **97**, 014906 (2018), [arXiv:1710.03329 \[nucl-th\]](#).
- [44] D. Everett, C. Chattopadhyay, U. Heinz, «Maximum entropy kinetic matching conditions for heavy-ion collisions», *Phys. Rev. C* **103**, 064902 (2021), [arXiv:2101.01130 \[hep-ph\]](#).
- [45] J.M. Luttinger, J.C. Ward, «Ground-State Energy of a Many Fermion System. II.», *Phys. Rev.* **118**, 1417 (1960).
- [46] G. Baym, «Self-Consistent Approximation in Many-Body Systems», *Phys. Rev.* **127**, 1391 (1962).
- [47] J.M. Cornwall, R. Jackiw, E. Tomboulis, «Effective action for composite operators», *Phys. Rev. D* **10**, 2428 (1974).
- [48] R.E. Norton, J.M. Cornwall, «On the formalism of relativistic many body theory», *Ann. Phys.* **91**, 106 (1975).
- [49] J. Berges, J. Serreau, «Progress in Nonequilibrium Quantum Field Theory», in: M.G. Schmidt (Ed.) «Strong and Electroweak Matter. Proceedings of the SEWM2002 Meeting», *Heidelberg, Germany, 2–5 October, 2002*, pp. 111–126.

- [50] M. Pradeep, K. Rajagopal, M. Stephanov, Y. Yin, «Freezing out fluctuations in Hydro+ near the QCD critical point», *Phys. Rev. D* **106**, 036017 (2022), [arXiv:2204.00639](#) [hep-ph].
- [51] NSAC, «A New Era of Discovery: The 2023 Long Range Plan for Nuclear Science», <https://nuclearsciencefuture.org/wp-content/uploads/2023/11/NSAC-LRP-2023-v1.3.pdf>, 2023.